Tohoku J. Exp. Med., 2000, **190**, 249-260

Visual Processing in Patients with Macular Hole

TETSUO HAMAMATSU, YOICHI NAKAGAWA, MAKOTO TAMAI and MASATOSHI ITO[1]

Department of Ophthalmology, Tohoku University School of Medicine, [1]Cyclotron and Radioisotope Center, Tohoku University, Sendai 980-8574

HAMAMATSU, T., NAKAGAWA, Y., TAMAI, M. and ITO, M. *Visual Processing in Patients with Macular Hole.* Tohoku J. Exp. Med., 2000, **190** (4), 249-260 —— Macular hole is a specific disease of the central retina that affects central visual acuity and central visual field. The purpose of this study is to investigate the alteration of visual processing in patients with macular hole who had small central scotoma. Six patients with macular hole participated in this study. We used positron emission tomography (PET) to measure task-related changes in regional cerebral blood flow to identify regions of the brain activated during visual stimulation. Three tasks were performed in each eye: control task, checkerboard task, shape-discrimination task. Checkerboard stimuli caused a greater blood flow activation response in normal eyes than in affected eyes at the occipital cortex. The area involved in the macular hole appeared to be 20 mm or more anteriorly from the occipital pole. The Shape-discrimination task in affected eyes activated angular gyrus, inferoparietal lobule, and middle frontal gyrus. Our findings demonstrated greater confidence in Horton's new retinotopic map than in Holmes' retinotopic map in cortical areas involved in macular function. The dorsal pathway of the visual system was activated more than the ventral pathway in patients with macular hole. ———— visual processing; PET; macular function; regional cerebral blood flow; Horton's retinotopic map

The previous studies of the visual system have tried to identify the retinocortical stream in humans. These studies were largely driven by a passive view of the visual stream that was thought to process the various attributes of different submodalities following visual response in primates (Boussaoud et al. 1990; Morel and Bullier 1990). Functional imaging of the human brain became available as a neuroscience tool because positron emission tomography (PET) had evolved into a mature technology. It was now possible to study complex visual processing in humans, which was difficult to investigate in primates (Orihara et al. 1997). The PET data obtained in humans can be compared not only with neurophysiological evidence, but also can be used as a new index to identify visual processing. In

Received January 17, 2000; revision accepted for publication March 15, 2000

Address for reprints: Tetsuo Hamamatsu, Department of Ophthalmology, Tohoku University School of Medicine, 1-1 Seiryomachi, Aoba-ku, Sendai 980-8574, Japan.

humans, most visual stimuli are transmitted by retinal cells along two separate neural pathways (Mishkin et al. 1983). Retinal ganglion cells supply retinal cells in the visual stream, which transmit visual information to the retina. It has been generally recognized that projection from the retina to the lateral geniculate nucleus (LGN) and to subcortical visual centers comprises several different functional classes of ganglion cells (Perry et al. 1984; Rodieck 1985). Evidence for the projections from the retina to the magnocellular and parvocellular stream has come from previous electrophysiological studies in primates, which demonstrated that parasol ganglion cells project to the magnocellular layers of LGN, whereas midget ganglion cells project to parvocellular layers. Furthermore parvocellular cells project mainly to sublamina 4cβ of the striate cortex, and magnocellular cells project mainly to sublamina 4cα (Merigan et al. 1991). Neurons in the magnocellular pathway have high contrast sensitivity, fast temporal resolution, and low spatial resolution and are color insensitive. Neurons in the parvocellular pathway have low contrast sensitivity, slow temporal resolution, and high spatial resolution and are color sensitive (Livingstone and Hubel 1987; Schiller et al. 1990; Van Essen and Gallant 1994). Each of these separate pathways conducts visual information from the retina to the striate cortex via a single synapse in the LGN. From the striate cortex, magno- and parvocellular neurons project to all extrastriate visual association areas (Maunsell and Nealey 1990; Ferrera and Nealey 1994; Nealey and Maunsell 1994).

Macular function is believed to contribute importantly to spatial resolution and color sensitivity in human visual perception, which has an almost parvocellular output. Macular hole is a disease of the central retina that affects central visual acuity and central visual field. The condition is due to tangential traction on the prefoveal cortical vitreous (Gass 1988). Gass (1995) has suggested a classification system, in which a stage I lesion is a premacular hole lesion, stage II lesion has early eccentric holes, and stage III and IV lesions are full-thickness macular holes. A full-thickness macular hole is a round break that involves all layers of the retina, from the internal limiting membrane through the outer segments of the photoreceptor layer (Funata et al. 1992; Madreperla et al. 1994). To investigate the visual processing of macular function, we identified the retinocortical stream with the regional cerebral blood flow (rCBF) activation in patients with macular hole related visual tasks. We used PET to measure task-related changes in (rCBF) activated during visual stimulation. The purpose of this study was to demonstrate the functional anatomy of the mechanisms involved in macular function in humans.

Methods

Subjects

Subjects were recruited from our macular hole study group in the department of ophthalmology, Tohoku University School of Medicine. We selected patients

who had unilateral macular hole and no other major medical disorder, as assessed by medical history, physical examination, chest X-ray, ECG, and laboratory test (complete blood counts; sedimentation rate, electrolytes, glucose, blood urea nitrogen, creatinine, liver-associated enzymes, cholesterol, triglycerides). Six patients (51–70 years old) participated in this study. All had unilateral macular hole and no visual abnormalities in the other eye as assessed by examinations (ophthalmoscopy, pupillary function, extraocular movement, acuity charts, and field integrity). All subjects gave written consent for participation after full explanation of the study. Patient characteristics are presented in Table 1. Five patients had stage IV macular holes and one patient had stage III.

TABLE 1. *Subject characteristics*

Subject No./ Age (year)/sex	Affected eye side/visual acuity	Fellow eye visual acuity	Duration of macular hole, mo	Classification of macular hole (Gass'stage)
1/75/F	L/0.1	0.9	12	IV
2/51/M	R/0.2	1.5	25	IV
3/67/F	L/0.04	1.0	18	III
4/60/M	R/0.2	1.2	4	IV
5/70/F	L/0.05	1.0	10	IV
6/61/F	L/0.1	0.3	6	IV

Visual stimulation

All the six subjects performed three tasks (control task; checkerboard task; shape-discrimination task). For all tasks, visual stimuli were presented on a head-mounted display (CE-LT14M Sharp Inc., Tokyo). The visual angle was set on 50°. The control task was performed on each subject inserted eye mask. In the checkerboard task, the frequency was reversed by 8 Hz on the monitor. Each subject was scanned three times in the checkerboard experiment. The same checkerboard task was given to the eye with macular hole, the contralateral normal eye, and both eyes. The shape-discrimination task was performed in only eyes with macular hole. In the shape-discrimination task, three differents shaped figures were shown on the monitor at random. These were an equilateral triangle, a regular square, and a circle each the same size by 7 cm and the same color. Subjects were asked to identify the regular square, and press a button with their right thumb when they saw it.

PET measurements

Each subject was placed comfortably in a supine position on a newly designed whole-body PET scanner (SET2400W, Shimadzu Inc., Tokyo) with a large axial field of view (Fujiwara et al. 1997). The rCBF was measured by using

^{15}O-labeled water. Transmission data of subjects in the same position were used to correct for attenuation with use of a 68Ge/Ga rotating source. After the intravenous administration of a bolus of 40 mCi ^{15}O-labeled water, the rCBF was measured for 100 seconds. The control task, checkerboard task, and shape-discrimination task were started before the bolus injection. Each PET measurement started immediately after radioactivity arrived within the PET field of view and was continued for a period of 100 seconds. Total counts per brain voxels during the build-up phase of radioactivity served as an estimate of rCBF. All PET images were smoothed with a three-dimensional 10-mm wide Gaussian filter, then normalized for global cerebral blood flow in milliliter • 100 g^{-1} • $minute^{-1}$. Functional imaging data analysis was based on the analytic method of statistical parametric mapping (Friston et al. 1994, 1995). We used SPM96b in this study. The images were registered, stereotaxically normalized into the space of the atlas, and smoothed in the X, Y, and Z axes (X = left/right, Y = posterior/anterior, and Z = inferior/superior). After the anatomic standardization of the rCBF images, we made voxel-by-voxel comparison pictures of the control from checkerboard and shape-discrimination task images for each subject. Then, mean and variance pictures and descriptive Student's t-statistic pictures for each comparison were calculated. In this study, voxels with $Z > 3.09$ ($p < 0.001$) were considered to represent regions of significantly changed rCBF in each visual stimulation task minus the control task image. After anatomic localization of activation in each comparison was made in relation to the mean reformatted MRI, the activated rCBF on both sides in primary visual cortex along calcarine fissure was calculated in each task to estimate the macular function.

Results

The comparison of the image, which was performed in normal eyes, eyes with macular hole, and both eyes minus control, was made to pick up the voxels showing statistically significant changes in rCBF in relation to macular function influenced by macular hole in human visual processing. The voxels showing statistically significant increases in rCBF were identified as the specific activation fields related to visual processing.

Fig. 1 identifies the brain areas in which rCBF showed increases in flash frequency at 8 Hz in both eyes. In comparison with the control task, the rCBF showed increasing responses in the posterior part that extended from the striate cortex inferiorly along the lingual and fusiform gyri and inferotemporal gyrus. Fig. 2 shows the areas of brain in which rCBF had increasing changes in flash frequency at 8 Hz in only the normal eye. In comparison with the control task, the rCBF showed increasing responses in the posterior part which extended from the striate cortex inferiorly along the lingual and fusiform gyri and inferotemporal gyrus, and in part of the right middle frontal gyrus. The significantly activated areas during checkerboard stimuli in the affected eye are shown in Fig. 3. In eyes

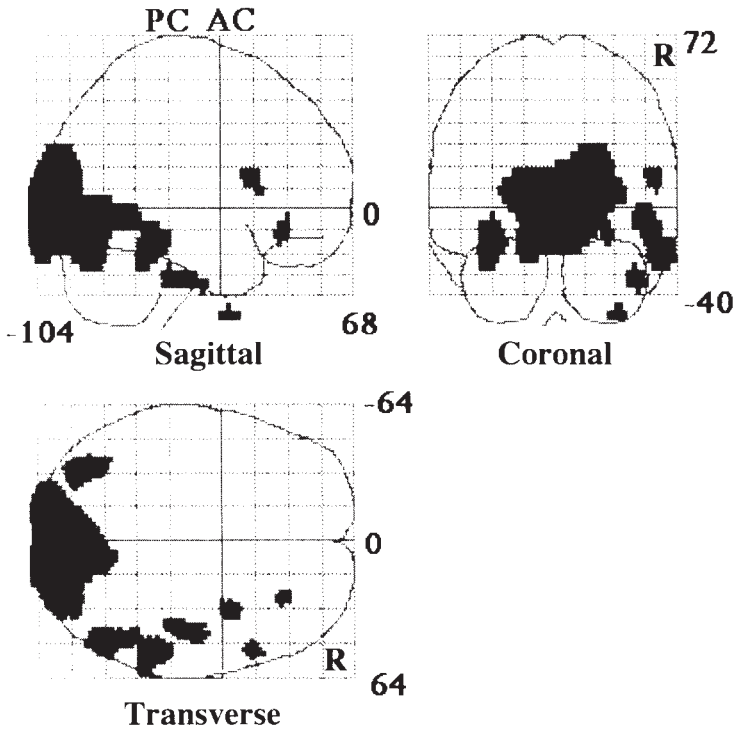

Fig. 1. Brain areas in which rCBF activated during visual stimulation of checkerboard task in both eyes. Grid numbers are millimeters relative to AC plane in sagittal projections, AC-PC plane in coronal projections, and midline sagittal plane in transverse projections.

The activation of rCBF was showed in the posterior part extended from the striate cortex inferiorly along the lingual and fusiform gyri and inferotemporal gyrus in comparison with the control task.

PC, posterior commissure; AC, anterior commissure; R, right side.

with macular hole, increasing rCBF were identified in ventral occipital cortex and inferotemporal cortex. The right middle frontal gyrus also had similar patterns in the normal eyes. An activated rCBF during the shape-discrimination task in eyes with macular hole is shown in Fig. 4. The increasing areas of rCBF were identified in inferotemporal gyrus, angular gyrus, inferoparietal lobule, and middle frontal gyrus, although there appeared to be less activation in the occipital cortex than observed in the checkerboard task.

In these experiments many visual foci were observed, especially when they performed significantly increasing responses in the primary visual cortex during checkerboard stimuli. In comparison with the activated cortical areas between the affected and normal eyes, the rCBF in primary visual cortex in each eye demonstrated characteristic differences, with regulated tendency for increasing responses during checkerboard stimuli. Fig. 5 identifies the activated degree on both sides in primary visual cortex along the calcarine fissure from the occipital pole to the anterior cortical area, during control, checkerboard, and shape-discrimination tasks in affected eyes, normal eyes, and both eyes. In the cortical area, about 6 mm anteriorly from the occipital pole in the checkerboard task, the activated rCBF in eyes with macular hole showed similar response patterns as in

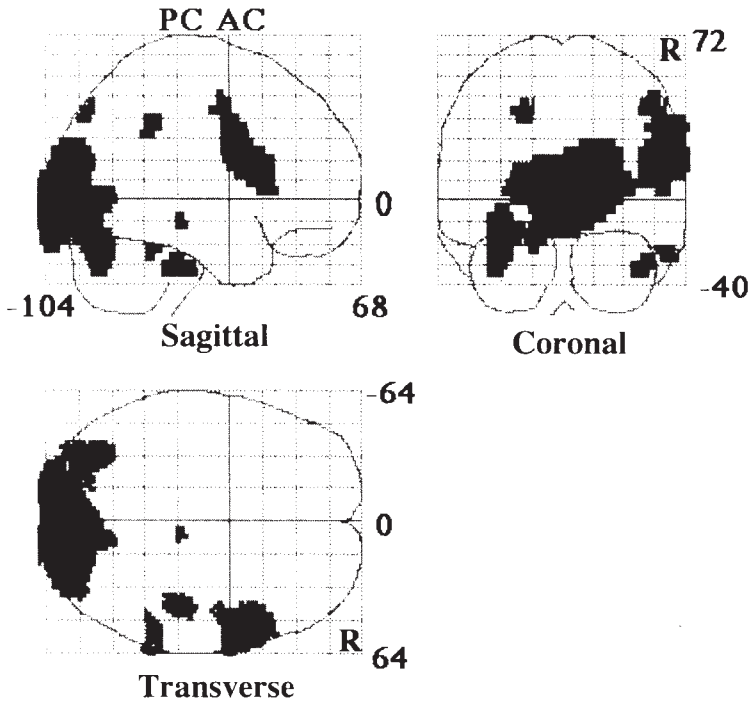

Fig. 2. Brain Areas in which rCBF activated during visual stimulation of checkerboard task in normal eyes. Grid numbers are millimeters relative to AC plane in sagittal projections, AC-PC plane in coronal projections, and midline sagittal plane in transverse projections.

The activation of rCBF was showed in the posterior part extended from the striate cortex inferiorly along the lingual and fusiform gyri and inferotemporal gyrus, and in part of the right middle frontal gyrus in comparison with the control task.

PC, posterior commissure; AC, anterior commissure; R, right side.

the normal eyes. However the activated rCBF in eyes with macular hole showed smaller responses near the occipital pole than in the normal eyes. Also, the activated rCBF in eyes with macular hole had greater response in the cortical area at 20 mm and more anteriorly from the occipital pole than in the normal eyes. In the shape-discrimination task, the activation in eyes with macular hole had no significantly different response anywhere from the occipital pole.

Discussion

The representation of the visual field in human striate cortex was studied by Holmes' who examined soldiers injured in the World War I and correlated visual field deficits of the occiput to the construct of the striate cortex (Holmes and Lister 1916; Holmes 1917). The Holmes' map had provided the most detailed source of primary data concerning the representation of visual field in the human striate cortex (Holmes 1945). In 1990, Horton and his colleague tested the accuracy of Holmes' retinotopic map of human striate cortex by correlating magnetic resonance scans with homonymous field defects in patients with clearly defined occipital lobe lesions (Horton and Hoyt 1991). They demonstrated that central vision occupies a greater proportion of human striate cortex than Holmes por-

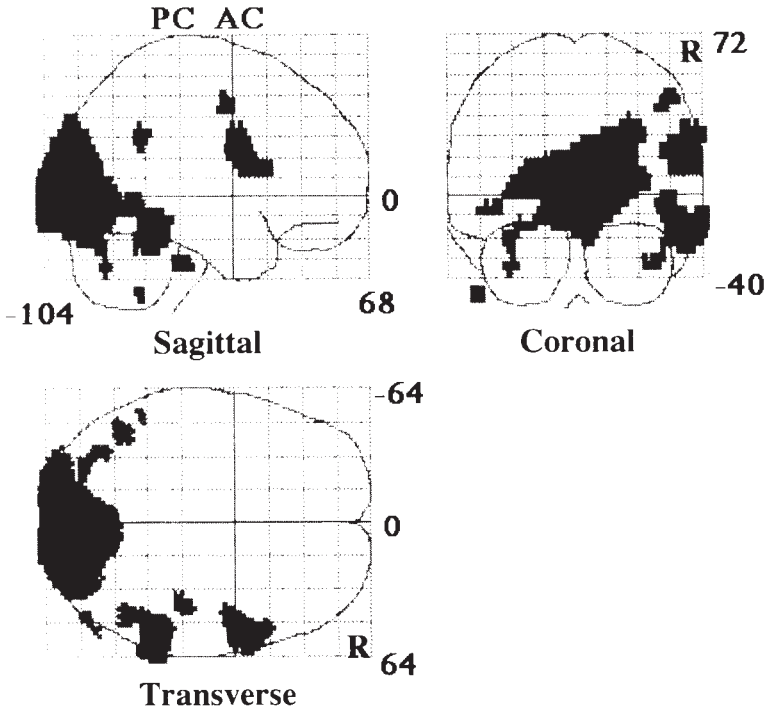

Fig. 3. Brain areas in which rCBF activated during visual stimulation of checkerboard task in eyes with macular hole. Grid numbers are millimeters relative to AC plane in sagittal projections, AC-PC plane in coronal projections, and midline sagittal plane in transverse projections.

The activation of rCBF was showed in ventral occipital cortex and inferotemporal cortex, and right middle frontal gyrus in comparison with the control task.

PC, posterior commissure; AC, anterior commissure; R, right side.

trayed. Macular sparing also should be carefully mapped using modern functional imaging methods in human visual system. Our study was conducted to determine where in the human brain visual pathway of macular function is processed in patients with macular hole.

The effects of checkerboard stimuli were shown significantly in primary visual cortex of eyes with macular hole and normal eyes. When a comparison was made of the activated cortical areas in each eye, the rCBF in primary visual cortex in each eye showed characteristic differences, with regulated tendency on the increasing responses during checkerboard stimuli. In eyes with macular hole, the activated rCBF showed smaller response in posterior visual cortex than in those with a normal eye, especially near the occipital pole. The rCBF response in normal eyes performed greater activation than eyes with macular hole according to the occipital pole in checkerboard stimuli. However, some interesting findings were seen along the striate visual cortex. The responses performed in eyes with macular hole were equal with those in normal eyes in the cortical area at about 6 mm or more anteriorly from the occipital pole. Also, greater activation was seen on eyes with macular hole in comparison not only with the normal eyes but also both eyes in the cortical area at 20 mm and more anteriorly from the occipital

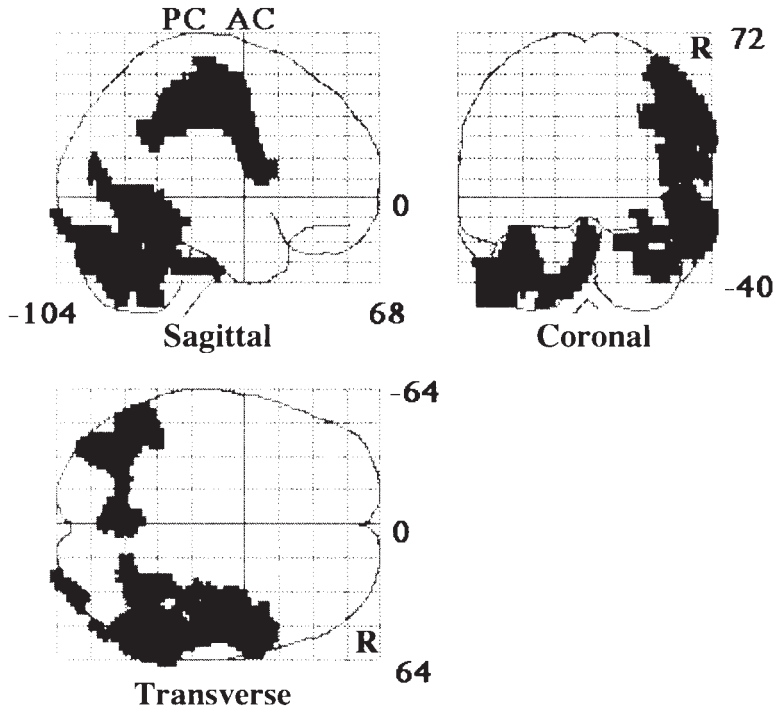

Fig. 4. Brain areas in which rCBF activated during visual stimulation of shape-discrimination task in eyes with macular hole. Grid numbers are millimeters relative to AC plane in sagittal projections, AC-PC plane in coronal projections, and midline sagittal plane in transverse projections.

The activation of rCBF was showed in inferotemporal gyrus, angular gyrus, inferoparietal lobule, and middle frontal gyrus in comparison with the control task.

PC, posterior commissure; AC, anterior commissure; R; right side.

Fig. 5. The degree of activated responses in eyes with macular hole, normal eyes, and both eyes on both sides in primary visual cortex along calcarine fissure from the occipital pole during control, checkerboard, and shape-discrimination tasks. (a: Control task, b: Checkerboard task in the both eyes, c: Checkerboard task in normal eyes, d: Checkerboard task in eyes with macular hole, e: Shape-discrimination task)

The cortical area at 24 mm anteriorly from the occipital pole
A (coordinates; 6, −80, 12), A'(coordinates; −6, −80, 12)
The cortical area at 20 mm anteriorly from the occipital pole
B (coordinates; 4, −84, 8), B'(coordinates; −4, −84, 8)
The cortical area at 6 mm anteriorly from the occipital pole
C (coordinates; 4, −98, −4), C'(coordinates; −4, −98, −4)
The cortical area at the occipital pole
D (coordinates; 4, −102, −4), D'(coordinates; −4, −102, −4)

In the cortical area, about 6 mm anteriorly from the occipital pole in the checkerboard task, the activated rCBF in macular hole eyes showed similar patterns with the responses in the normal eyes. However the activated rCBF in eyes with macular hole showed a smaller response near the occipital pole than the normal eyes. Also, it had greater response in the cortical area at 20 mm and more anteriorly from the occipital pole. In shape-discrimination task, the activation in macular hole eyes had no significantly different response anywhere from the occipital pole.

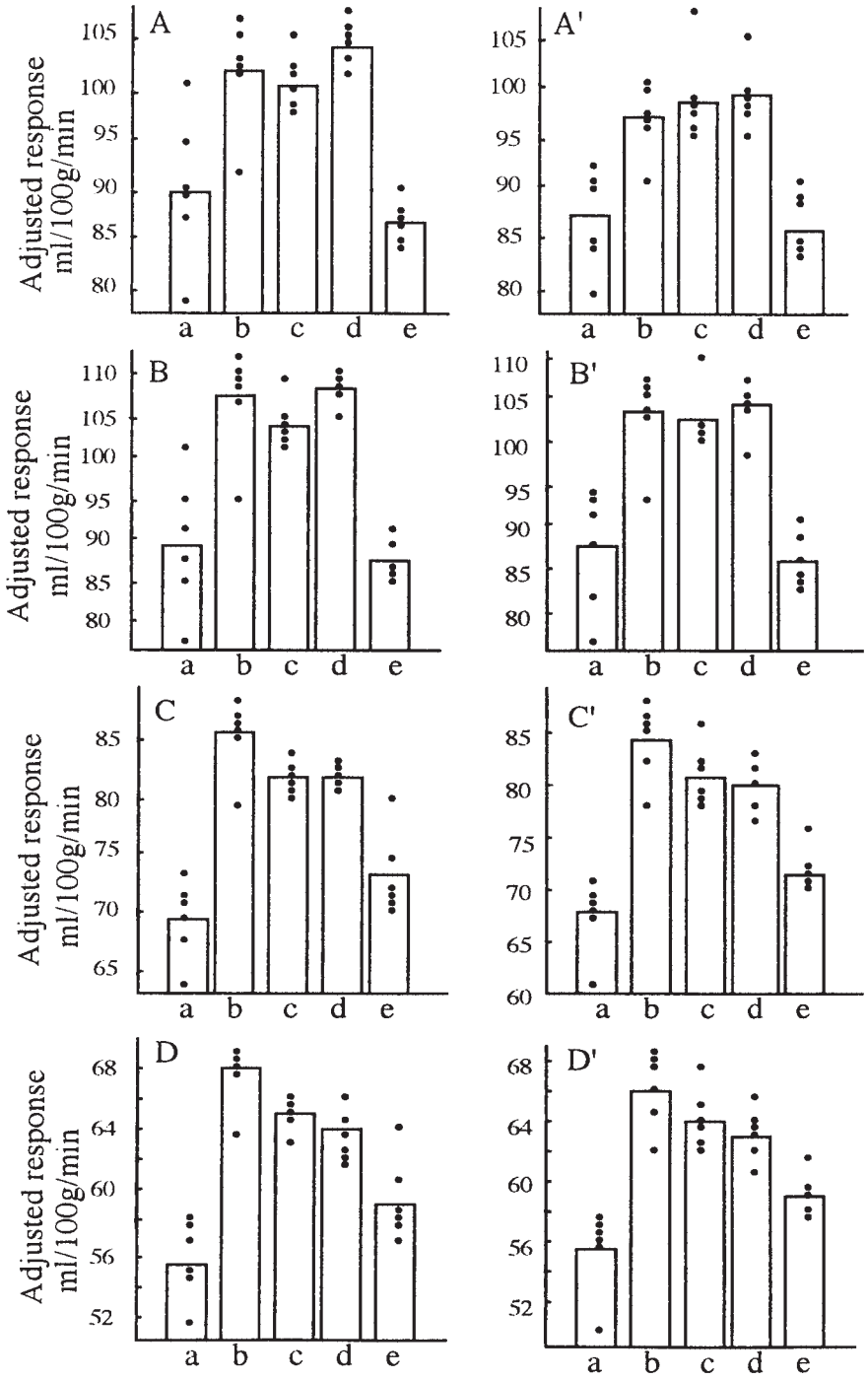

Fig. 5.

pole. These activating changes in the areas identify the interaction of visual processing involved in increased peripheral macular function instead of the affected central visual function, and relatively assured smaller responses in areas posteriorly from the reversed region involved in central macular function influenced by macular hole. These results demonstrate the mapping of the cortical areas involved in macular function in human visual processing. The projected cortical area of macular hole might correspond to the posterior area at least in 20 mm and more anteriorly from the occipital pole. They further suggested greater confidence of Horton's retinotopic map over Holmes' map in cortical areas involved in macular function.

In the shape-discrimination task, eyes with macular hole showed activated responses in angular gyrus, inferoparietal lobule, and prefrontal visual cortex that appeared less than in the occipital cortex. Previous experimental data have suggested that the parietal cortex might be involved in some aspects of shape discrimination (Faillenot et al. 1997). Recently, Goodale and Milner (1992) reported that a re-evaluation of the functional distinction between the two cortical visual streams has been prompted. Both streams would process visual information about object orientation and shape, but each stream would use it to achieve different goals. The ventral stream plays a critical role in the visual perception of objects, while the dorsal stream mediates the sensorimotor transformations required for visually guided action directed toward them (Goodale and Milner 1991). Our results might correspond with motion vision in dorsal pathway of visual system, because visual processing in patients with macular hole who had a specific condition with small central scotoma might indicate searching for a shaped index on the monitor. For this reason, the magnocellular pathway in visual system might be activated more than parvocellular pathway in eyes with macular hole. If it was possible to compare the data in affected and normal eyes during the shape-discrimination task, the other mechanisms of visual processing involved in macular function might be demonstrated, and identified new order in objective recognition.

References

1) Boussaoud, D., Ungerleider, L.G. & Desimone, R. (1990) Pathways for motion analysis: cortical connections of the medial superior temporal and fundus of the superior temporal visual areas in the macaque. *J. Comp. Neurol.*, **296**, 462-495.
2) Faillenot, I., Toni, I., Decety, J., Gregoire, M.C. & Jeannerod, M. (1997) Visual pathways for object-oriented action and object recognition: Functional anatomy with PET. *Cerebral Cortex*, **7**, 77 85.
3) Ferrera, V.P. & Nealey, T.A. (1994) Responses in macaque visual area V4 following inactivation of the parvocellular and magnocellular LGN pathways. *J. Neurosci.*, **14**, 2080-2088.
4) Friston, K.J., Worsley, K.J., Frackowiak, R.S., Mazziotta, J.C. & Evans, A.C. (1994) Assessing the significance of focal activations using their statistical extent. *Human Brain Mapping*, **1**, 210-220.

5) Friston, K.J., Holmes, A.P., Worsley, K.J., Poline, J.B., Frith, C.D. & Frackowiak, R. S. (1995) Statistical parametric map in functional neuroimaging: A general linear approach. *Human Brain Mapping*, **2**, 189-210.
6) Fujiwara, T., Watanuki, S., Miyake, M. & Ito, M. (1997) Performance evaluation of a large axial field-of-view PET scanner. *Ann. Nuclear Med.*, **11**, 307-313.
7) Funata, M., Wendel, R.T., de la Cruz, Z. & Green, W.R. (1992) Clinicopathologic study of bilateral macular holes treated with pars plana vitrectomy and gas tamponade. *Retina*, **12**, 289-298.
8) Gass, J.D.M. (1988) Idiopathic senile macular hole. *Arch. Ophthalmol.*, **106**, 629-639.
9) Gass, J.D.M. (1995) Reappraisal of biomicroscopic classification of stages of development of a macular hole. *Am. J. Ophthalmol.*, **119**, 752-759.
10) Goodale, M.A. & Milner, A.D. (1991) A neurological dissociation between perceivingobjects and grasping them. *Nature*, **349**, 154-156.
11) Goodale, M.A. & Milner, A.D. (1992) Separate visual pathways for perception and action. *Trends. Neurosci.*, **15**, 20-25.
12) Holmes, G. & Lister, W.T. (1916) Disturbances of vision from cerebral lesions with special reference to the cortical representation of the macula. *Brain*, **39**, 34-73.
13) Holmes, G. (1917) Disturbances of vision by cerebral lesion. *Br. J. Ophthalmol.*, **2**, 353-384.
14) Holmes, G. (1945) The organization of the visual cortex in man. *Proc. R. Soc. Lond. Series Biol.*, **132**, 348-361.
15) Horton, J.C. & Hoyt, W.F. (1991) The representation of the visual field in human striate cortex. A revision of the classic Holmes map. *Arch. Ophthalmol.*, **109**, 816-824.
16) Livingstone, M.S. & Hubel, D.H. (1987) Psychophysical evidence for separate channels for the perception of color, movement and depth. *J. Neurosci.*, **7**, 3416-3468.
17) Madreperla, S.A., Geiger, G.L., Funata, M., de la Cruz, Z. & Green, W.R. (1994) Clinicopathologic correlation of a macular hole treated by cortical vitreous peeling and gas tamponade. *Ophthalmology*, **101**, 682-686.
18) Maunsell, J.H.R. & Nealey, T.A. (1990) Magnocellular and parvocellular contributions to responses in the middle temporal visual area(MT) of the macaque monkey. *J. Neurosci.*, **10**, 3323-3334.
19) Merigan, W.H., Katz, L.M. & Maunsell, J.H.R. (1991) The effects of parvocellular lateral geniculate lesions on the acuity and contrast sensitivity of macaque monkeys. *J. Neurosci.*, **11**, 994-1001
20) Mishkin, M., Ungerleider, L.G. & Macko, K.A. (1983) Object vision and spatial vision: two cortical pathways. *Trends. Neurosci.*, **6**, 414-417.
21) Morel, A. & Bullier, J. (1990) Anatomical segregation of two cortical visual pathways in the macaque monkey. *Vis. Neurosci.*, **4**, 555-578.
22) Nealey, T.A. & Maunsell, J.H. (1994) Magnocellular and parvocellular contributions to the responses of neurons in macaque striate cortex. *J. Neurosci.*, **14**, 2069-2079.
23) Orihara, H., Ishii, K., Iwata, R., Fujiwara, T. & Itoh, M. (1997) Three-dimensional positron emission tomography imaging system and its application for medical use. *Jpn. J. Clin. Med.*, **55**, 2148-2155.
24) Perry, V.H., Oehler, R. & Cowey, A. (1984) Retinal ganglion cells which project to the dorsal lateral geniculate nucleus in the macaque monkey. *Neuroscience*, **12**, 1101-1123.
25) Rodieck, R.W. (1985) Parasol and midget ganglion cells of the human retina. *J. Comp. Neurol.*, **233**, 115-132.
26) Schiller, P.H., Logothetis, N.K. & Charles, E.R. (1990) Functions of the colour-opponent and broadband channels of the visual system. *Nature*, **343**, 68-70.

27) van Essen, D.C. & Gallant, J.L. (1994) Neural mechanisms of form and motion processing in the primate visual system. *Neuron*, **13**, 1–10.